Ion Storage Tests With The High Performance Antiproton Trap (HiPAT)

James Martin[1], Raymond Lewis[2], Suman Chakrabarti[1] and Boise Pearson[1]

[1]*NASA MSFC, TD40, Huntsville, Alabama, 35812*
[2]*R. Lewis Company (MSFC, TD40), Huntsville, Alabama, 35812*
James.J.Martin@msfc.nasa.gov / (256) 544-6054 / Fax (256) 544-5926

Abstract. The matter antimatter reaction represents the densest form of energy storage/release known to modern physics: as such it offers one of the most compact sources of power for future deep space exploration. To take the first steps along this path, the NASA-MSFC is developing a storage system referred to as the High Performance Antiproton Trap (HiPAT) with a goal of maintaining 10^{12} particles for up to 18 days. Experiments have been performed with this hardware using normal matter (positive hydrogen ions) to assess the device's ability to hold charged particles. These ions are currently created using an electron gun method to ionize background gas; however, this technique is limited by the quantity that can be captured. To circumvent this issue, an ion source is currently being commissioned which will greatly increase the number of ions captured and more closely simulate actual operations expected at an antiproton production facility. Ions have been produced, stored for various time intervals, and then extracted against detectors to measure species, quantity and energy. Radio frequency stabilization has been tested as a method to prolong ion lifetime: results show an increase in the baseline 1/e lifetime of trapped particles from hours to days. Impurities in the residual background gas (typically carbon-containing species CH_4, CO, CO_2, etc.) present a continuing problem by reducing the trapped hydrogen population through the mechanism of ion charge exchange.

INTRODUCTION

To undertake many of the aggressive deep space missions envisioned in the future, new high energy density propulsion will be required so that mission timelines can be measured in years instead of decades to centuries. One source for this incredible quantity of energy is that of antimatter and the annihilation energy that it represents. This process provides 10^8 MJ/g (proton-antiproton reaction) providing approximately 10 orders of magnitude more energy density than chemical systems currently used by NASA and the commercial launch vehicle market. Potential schemes conceived to use this exotic energy range from the simplest approach—which approximates the operation of nuclear thermal reactor—to the ultimate design of the beam core or pion engine (Vulpetti, 1984; Morgan, 1982; Rider 1997). A more attractive near term approach will most certainly be a hybrid concept that uses a combination of antiprotons and fission/fusion fuels to power a propulsion system. These hybrid systems need far fewer antiprotons when compared to other antiproton-based approaches, with requirements ranging from nanograms to milligrams (Gaidos, 1998; Kammash, 1992; Perkins, 1999). In addition to propulsion applications, there are near-term commercial uses of antiprotons related to the production of medical radioisotopes, and tumor diagnosis and treatment (Howe, 1988). Antiproton requirements for these commercial applications and testing of propulsion concepts are well within the current production capability at a facility such as the Fermi National Acceleration Laboratory (Schmidt, 2000). For all these potential commercial and propulsion applications, antiproton storage is a fundamental enabling technology. To address this key area, a hardware-based test program was initiated by the Marshall Space Flight Center (MSFC) to fabricate and test a functional trap system, referred to as the High Performance Antiproton Trap (HiPAT). Its objectives are to hold up to one trillion antiprotons with a storage lifetime of approximately 18 days (Martin, 2001). This basic hardware system has been completed and test evaluation is continuing using normal matter ions to simulate antiprotons. These ions are produced by two methods: 1) an electron gun that generates ions from residual background gas within the trap, and 2) an external ion source, which generates the ions and then transports them into the trap (more representative of antimatter operations). HiPAT is also being designed around a portable architecture since the production and utilization sites will in most cases not coincide.

TRAP HARDWARE DESCRIPTION

Figures 1 and 2 illustrate the basic layout of the HiPAT hardware as set up in the MSFC laboratory. There are a number of subsystems including a superconducting magnet, ultra high vacuum pumping equipment, high voltage electrode assembly, and electronics to monitor/interact with trapped particles. The entire system is designed around portability, adding flexibility that allows it to be integrated with fixed devices such as the ion source as well as preparing it for operation at an antiproton production facility. All power is provided through a set of large portable battery backup units, which allow up to 10 hours of autonomous operation. The magnet is a 4 Tesla superconducting arrangement (using liquid nitrogen and helium) with an end-compensated solenoid designed to maximize field uniformity along the central bore. This maximum field provides significant margin above the 1 Tesla requirement to meet one of the program objectives (as shown in Figure 3). This magnet is equipped with a cryogenic cooler (to minimize fluid consumption) and an active magnetic shield to limit the magnetic field extending beyond the Dewar boundary (simplifying laboratory operation). The vacuum arrangement consists of an oil-free system using dry scroll pumps to back turbo pumps providing operation to 10^{-10} torr. For operation in the 10^{-11} torr range and below, the system is additionally equipped with ion pumps (fitted with non-evaporable getters) and titanium sublimation pumps.

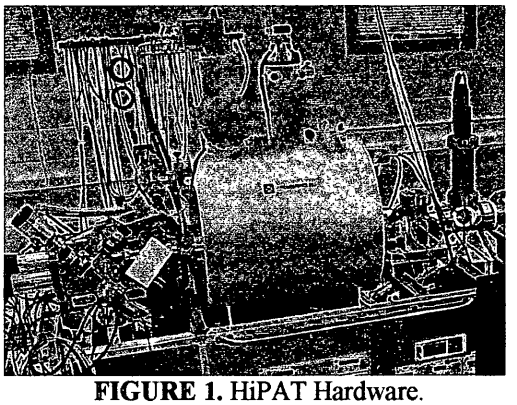

FIGURE 1. HiPAT Hardware.

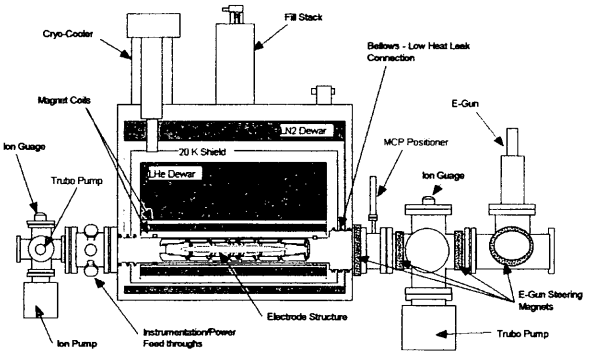

FIGURE 2. HiPAT Schematic.

The electronics systems incorporated into HiPAT are used to detect, monitor and interact with the trapped particles. These components are located external to the trap system, using vacuum feedthroughs and transmission lines to send and receive signals from the electrode structure within the vacuum. This electrode structure consists of titanium cylinders held in place and insulated from the surrounding beam line by a Macor exoskeleton (Figure 4). There are 6 primary single element electrodes, and 2 pick-up rings composed of 4 elements each. This electrode array measures 6 cm in diameter and 40 cm in length and completely encloses the confinement space. The electrode assembly is capable operating at up to 20 kV (electrodes 1 and 6), a necessity to achieve the project goal of holding 10^{12} charged particles (cf. Figure 3).

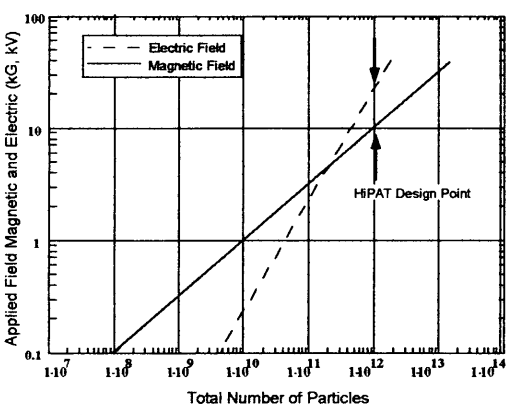

FIGURE 3. HiPAT Design Point.

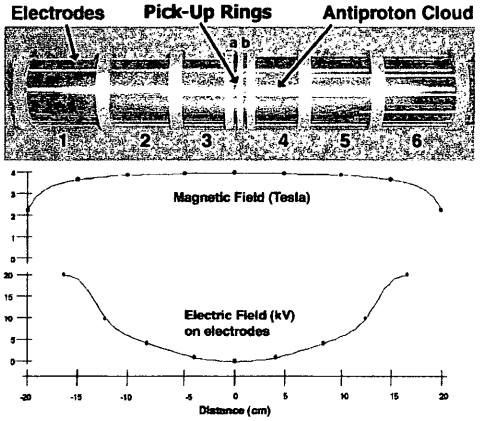

FIGURE 4. HiPAT Electrode Assembly.

ION PRODUCTION METHODS

The ultimate test of HiPAT's overall performance will be to assess its functionality with antiprotons. As a precursor to this activity, the system can be evaluated with normal matter ions such as positively and negatively charged hydrogen ions. The use of normal matter ion beams significantly simplifies evaluation since they are low cost, easy to obtain, and can be operated at will to provide a wealth of applicable experimental test data. More importantly however, using low energy normal matter beams eliminates the risk of radiation or material activation hazards present when using antiprotons. These normal matter based techniques can be used to accurately test particle containment, injection/extraction, and detection/stabilization methodology and hardware. They cannot directly address issues related to annihilation losses.

Electron Gun System

The simplest or "poor man's" approach to injecting ions in the HiPAT is through ionization of background gas within the electromagnetic well itself to in effect create the ions in the correct location "on the fly". This method is attractive in that it is both relatively simple to set up and operate and requires no special timing or dynamic cycling of the trap's electric field. The procedure entails injecting electrons into a "positive" potential well generated via the HiPAT electrodes. After ionizing the background gas, these primary electrons collide with a stainless steel screen positioned beyond the potential well. The purpose of the screen is twofold: 1) measuring the total electron current (verify beam focus); and 2) as a source of gas for the ionization process (gases desorbed by electron beam collision). The simplicity of this system makes it ideal for initial checkouts and simple experimentation since it significantly eases hardware operations. However, the lower number of "trappable" ions that can be produced limits this technique.

The collision of primary electrons with background gas results in ionization and creation of secondary electrons, resulting in further ionization through a process referred to as pigging (Wolf, 1995):

$$e^- + H_2 \rightarrow H + H^+ + 2e^- \quad \text{and} \quad e^- + H_2 \rightarrow H^- + H^+ + e^-$$

The number of ions produced is proportional to the product of the background gas density (n), the interaction cross-section (σ), the production path length (L), and the total number of primary electrons (e); it can be expressed as:

$$Ions_{total} = n\ \sigma\ e_{total}\ L_{path}$$

Typical electron gun parameters used with HiPAT consist of 10 μamps of current for several seconds resulting in the production of several millions of ions within the potential well. However, very few of these ions are actually trapped since the axial confinement field is severely limited by the minuscule production volume swept out by the electron beam. This beam is compressed by the strong central magnetic field to a diameter of 30 microns over the critical production length of approximately 15 cm. With electric potentials of 2 kV (limited to prevent Penning glow discharge at higher voltages), this thin filament can confine a maximum of 75,000 ions before they begin escaping axially. Typical tests of the HiPAT system are on the order of 1 kV (to provide an additional margin against discharge), resulting in ion production of approximately 40,000 ions, as measured by a micro-channel plate detector immediately after production. An additional escape mechanism involves creation of a potential hole in the trap's electric field as the primary electron beam enters (charge shielding).

Ion Source Method

The use of an external ion source provides the capability to fill HiPAT in a way similar to that expected at an actual production facility. Operation of this system is more complex than that of the electron gun because it requires both active transport of the ions and dynamic control of the trap's electric potential to capture a segment of the incoming beam. Unlike the electron gun technique, this approach can be used to accumulate multiple ion shots (referred to as stacking) through sequential cycling of source, beam line and the HiPAT trap. The ion source currently being commissioned has a maximum energy of 20 keV with a beam current in excess of 100 μamps above 8 kV. The beam line that connects the source to HiPAT serves a dual purpose: 1) transport of the ions using electrostatic lensing for focusing, and 2) providing for differential pumping of the vacuum system enabling the source to operate at 10^{-6} torr and the trap at 10^{-11} torr or less. These sources are illustrated in Figure 5. From bench testing, the

measured beam current will provide an ion single shot/stack capture baseline as shown in Figure 6. There is potential to improve the number of trapped ions per shot by raising the interior electrode voltages to nearly the level of the exterior electrode voltages. This procedure temporarily flattens the potential well during the injection period (reducing the relative energy of the incoming beam): the ions move more slowly, therefore residing longer inside the trap. The expected performance for this operation is also illustrated in figure 6; nominal performance should place between 10^7 and 10^9 ions per stacking event into the HiPAT at beam energy of 10 keV.

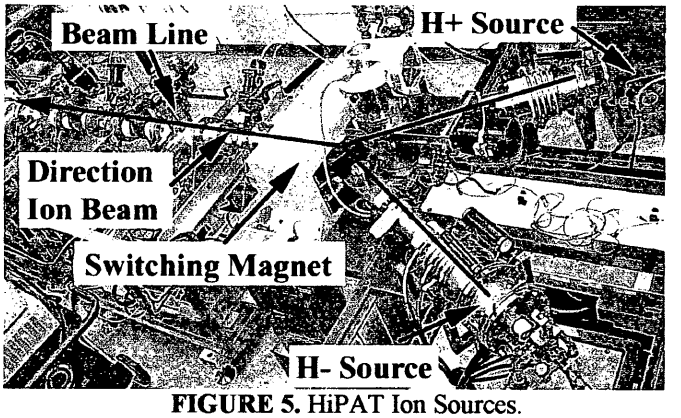

FIGURE 5. HiPAT Ion Sources.

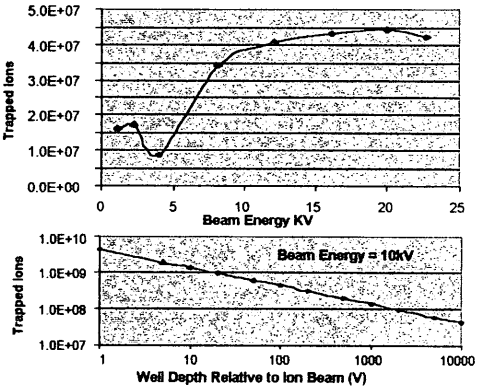

FIGURE 6. Estimated Ion Capture.

COMPUTATIONAL MODELING

Computational modeling of charged particles injected into the HiPAT system can assist in predicting the behavior of said particles. For example, Figure 7 shows the interference from oscillating electrons in a particular trap electrode voltage configuration (see next section): the observed frequency is 40.355 MHz. The number of contained particles is estimated at 10^8 (much higher than expected by electron gun injection) as a result of Penning discharge, which tends to rapidly fill the negative well with electrons. Their aggregate behavior can be approximated to first order via use of a code that determines motion of charged particles in a combination of electrostatic and magnetostatic fields. The code used, TRAPEX, has been extended and modified through a number of revisions from its origin—the SLAC electron gun design code called EGUN (Herrmansfeldt, 1988). Given HiPAT's static magnetic field and a given configuration of trap electrode voltages (see next section), TRAPEX solves Laplace's equation to obtain the electric potential and field (see Figure 8). TRAPEX can then trace individual particle trajectories via a fourth-order Runge-Kutta solution of the Lorentz force equation. The electrode voltages are chosen to form a roughly quadratic potential well: this means that a simple harmonic oscillator approximation can be used to estimate the oscillation frequency of charged particles in that electrostatic field. For Figure 8, the predicted electron oscillation frequency is 40.3 MHz, or a tiny fraction of a percent from the experimental observation. Such predictive capabilities make it easier to anticipate frequencies of different particles in diverse experimental configurations. More detailed modeling using a UC-Berkeley plasma PiC code (XOOPIC) is being initiated (Verboncoeur, 1995).

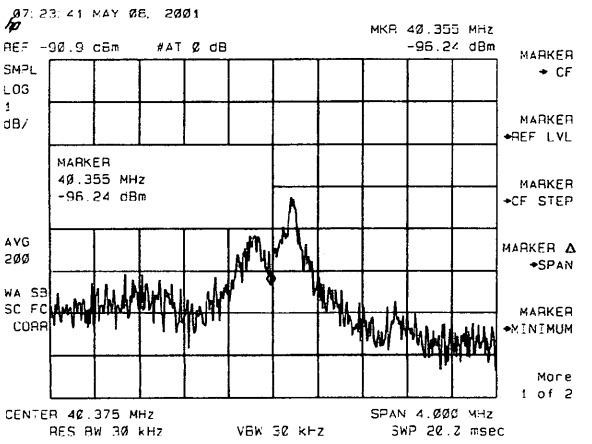

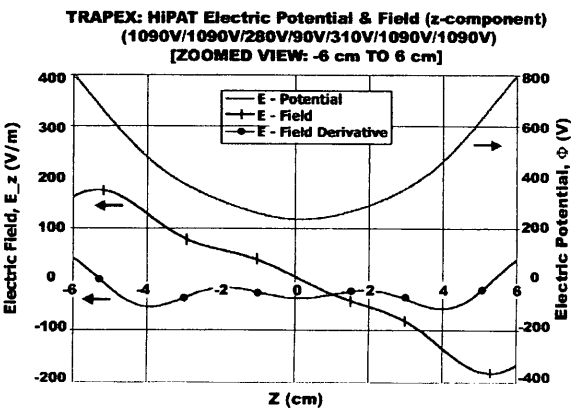

FIGURE 7. Electron Oscillation Frequency

FIGURE 8. HiPAT Electric Potential & Field

RESULTS

Experiments performed to date have focused on the storage of positive hydrogen ions. Limited testing has examined negative hydrogen ion and electron storage within a negative well configuration but will not be discussed. The primary goal was the determination of HiPAT's baseline lifetime performance with the few trappable ions that can be produced. Particle detection for these evaluations made use of a destructive extraction technique employing a microchannel plate (MCP) device located approximately 45cm from the trap center. This system is contrasted by a passive approach that monitoring signals produced by the trapped ions (using the 4 segmented pickup ring and spectrum analyzer). However, the passive signals were insufficient due to the small number trapped and hence unreliable as a means of assessing performance.Typical maximum operating voltages for the potential well during these tests ranged from 1 to 1.5 kV, set below the upper value of 2 kV to reduce the likelihood of generating a Penning glow discharge (which becomes evident via large signals on the spectrum analyzer). Additionally, the use of radio frequency (RF) stabilization has been extensively tested using 4 segments of a pickup ring to impose a rotating wall (Hollmann, 2000) phasing pattern (0, 90, 180, and 270 degrees) of the desired frequency. Experiments examined the potential benefits of RF on both particle lifetime and charge exchange. For all testing discussed, a nearly harmonic potential was established. Voltages on electrodes 1 through 6 were set to 1090, 1090, 280, 310, 1090, and 1090 volts, respectively—the dual pickup ring was maintained at approximately 90 volts. The inner well is slightly asymmetric around the trap center to maintain an additional accelerating potential for rapid extraction of ions from the trap. Typical vacuum levels as measured by ionization gauges in the forward pumping manifold ranged from $8x10^{-11}$ to $1x10^{-10}$ torr during storage intervals and reached a maximum transient pressure of $3x10^{-10}$ torr when the electron gun was fired. For all tests discussed the superconducting magnet was operated at approximately 2.2 Tesla, roughly half its maximum value.

Baseline storage performance is shown in the particle extraction sequence illustrated in Figure 9. To minimize the impact of human errors on the repetitive nature of these tests, a programmable logic controller was used to control injection, hold and extraction sequences. As expected, the electron beam produced approximately 42,000 hydrogen ions—an amount roughly constant for all test sequences. It is noted that ion exchange occurs quite rapidly during the storage interval; therefore all lifetime calculations are based on total charges (all species) contained within the trap rather than specific species. The ions decayed away rapidly during the first 10 minutes, exhibiting a high infant mortality rate with a 1/e lifetime of approximately 655 seconds as defined by:

$$\tau = (d \log(N)/dt)^{-1}$$

For the remainder of the 40-hour test interval (after the initial 10 minutes), this 1/e lifetime increased to a nearly constant value of 30,000 seconds. As a crosscheck, a model of radial diffusion (Bollen, 1996) can be used to relate the ion lifetime with background gas density:

$$\tau = 1/(n\,\sigma\,v) * (f_c/f_z)^2$$

where n is the background density, σ the elastic scattering cross section, v the speed of the ions, f_c and f_z the cyclotron and axial frequencies. A pressure of $1x10^{-10}$ Torr in the beam line at 300 K corresponds (Roth, 1988) to a steady-state density of $n=8.1*10^6$ molecules/cm^3 in the trap at 60 K. The scattering cross section is estimated as $\sigma=10^{-15}$ cm^2. The ion energy is estimated as 0.038 eV, from the variation in space charge potential in a cloud of 2700 CO^+ ions (primary charge remaining) at the Brillouin density. The cyclotron and axial frequencies for a CO^+ ion are $f_c=1.19$ and $f_z=0.18$ MHz. These estimated parameters imply a lifetime of 89,000 seconds. Thus, the radial diffusion model explains the observed lifetime within a factor of three, which is comparable to uncertainties in factors such as the cross section and ion energy.

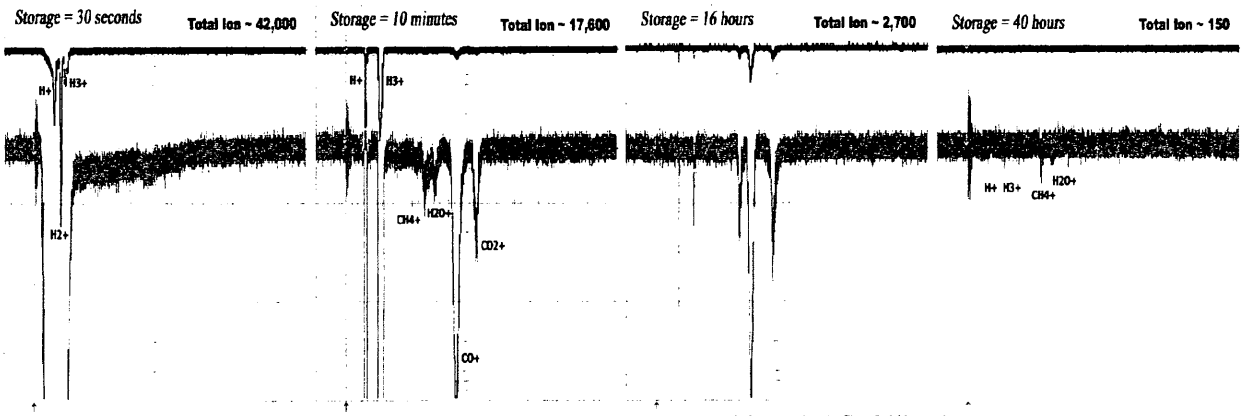

FIGURE 9. HiPAT Baseline Ion Storage (without RF Stabilization).

Upon completion of the baseline series, the RF rotating wall stabilization technique was implemented. These experiments examined a number of frequencies and signal amplitudes; the most promising range was found in the 400 to 500 kHz range with an amplitude ranging from -20 to 0 dBm. Figure 10 illustrates this benefit with a storage sequence performed identically to baseline tests with the exception of RF addition. One first notes that ion chemistry has not been significantly affected; however lifetime is noted to have increased. The 1/e lifetime is enhanced over the first 40 hours, approaching a value of 100,000 seconds—a factor of 3.3 higher than the similar baseline average. However, a significant observation is that lifetime increases substantially beyond the 40-hour mark: the recorded ion data shows little loss of charge during this period with a resulting 1/e lifetime of 400,000 seconds. Figure 11 shows this experimental result, presenting total ion counts and corresponding lifetimes for each interval. These RF results demonstrate precisely the effect being sought to achieve the 18-day storage goal.

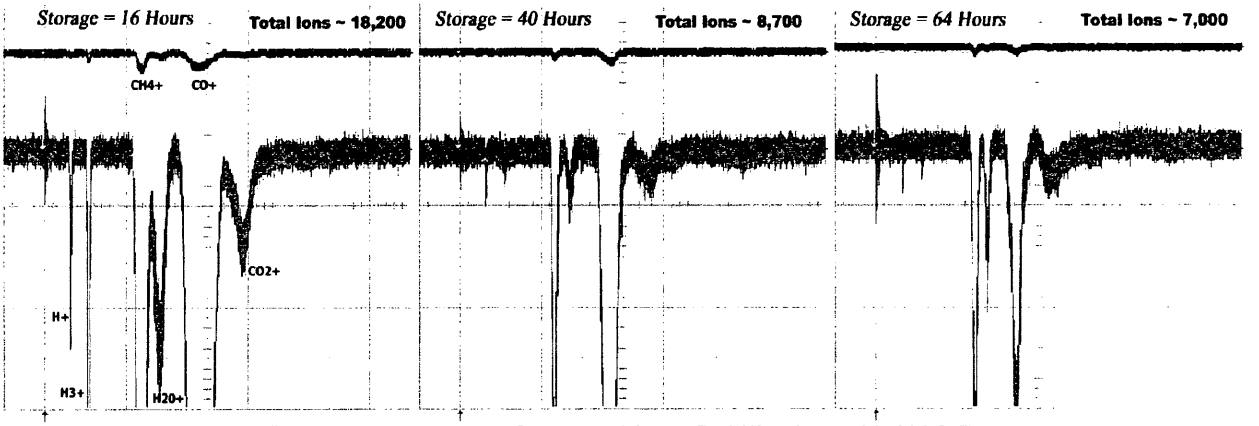

FIGURE 10. HiPAT Ion Storage with RF Stabilization (400-500 MHz).

Additional testing examined the effects of high frequency cyclotron excitation on stored ions using the rotating wall technique. Specific cyclotron frequencies for each of the stored ion species were calculated (as functions of magnetic field intensity) and then applied over a storage period of approximately 600 seconds. The effect of this RF on the trapped ions is dramatically illustrated in Figures 12 and 13. It is readily apparent from the time of flight extraction data that as RF was applied to a particular ion species, that species was removed from the trapping volume. These cyclotron excitation bands were fairly narrow and were swept continuously with output amplitudes ranging from -20 to 0 dBm using a frequency generator. During the highest frequency RF tests—applied to excite the hydrogen ions—it was noticed that H_2^+ (which is normally absent) suddenly appears in counts as high as 1000 ions during H_3^+ excitation and counts up to 100 ions while exciting the H^+ band. Furthermore, during hydrogen RF excitation there appears to be a slight enhancement of the ion charge exchange process yielding more of the heavier ion species. It is noted that all cyclotron frequency band tests to date have produced no lifetime increase of any trapped species. However, cyclotron heating applied to slightly different trap geometry has been reported (Bollen, 1996) to compress and maintain ion clouds.

Howe, S.D., "Portable Pbars, Traps that Travel", Los Alamos National Laboratory Report, LA-UR 88-737, 1988

Kammash T., and Galbraith, D.L., "Antimatter-Driven Fusion Propulsion Scheme for Solar System Exploration," *Journal of Propulsion and Power*, Vol. 8, No. 3, May 1992

Martin, J. J., et. al., "Design and Preliminary Testing of a High Performance Antiproton Trap (HiPAT)," STAIF-2001, 2001

Morgan, D.L., "Concepts for the Design of an Antimatter Annihilation Rocket," *J. British Interplanetary Society*, Vol 35.9, 1982

Perkins, L.J., "Antiproton Fast Ignition for Inertial Confinement Fusion," Fusion Technology, Vol. 36, pp 219-233, Sept 1999

Rider, T.H., "Fundamental Constraints on Large-Scale Antimatter Rocket Propulsion," *Journal of Propulsion and Power*, Vol. 13, Nov 3, 1997

Roth, A., "Vacuum Technology," North-Holland Publishing Company, 1976

Schmidt, G.R., et. al., "Antimatter Production and Energy Costs for Near-Term Propulsion Applications," *Journal of Propulsion and Power*, Vol.16, No. 5, 923-928, 2000

Wolf, B., "Handbook of Ion Sources", CRC Press, Boca Raton, 1995.

Verboncoeur, J.P., et. al., "An Object-Oriented Electromagnetic PIC Code", Comp. Phys. Comm., 87, May11, 1995, pp. 199-211.

Vulpetti, G. "A Propulsion-Oriented Synthesis of the Antiproton-Nucleon Annihilation Experimental Results", *J. British Interplanetary Society*, 37 (1984), pp. 124-134.